Electronic Supplementary Information
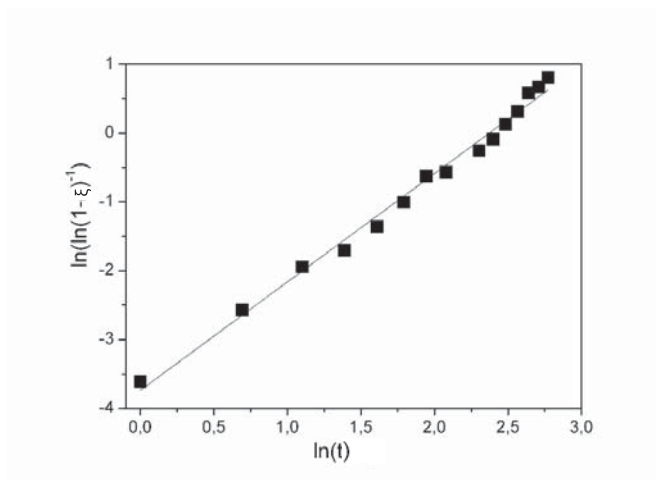

Fig. S1 Fit of the experimental data for the growth of the needle-shaped crystal through Avrami-Erofee'v model ($R^2 = 0.99022$).
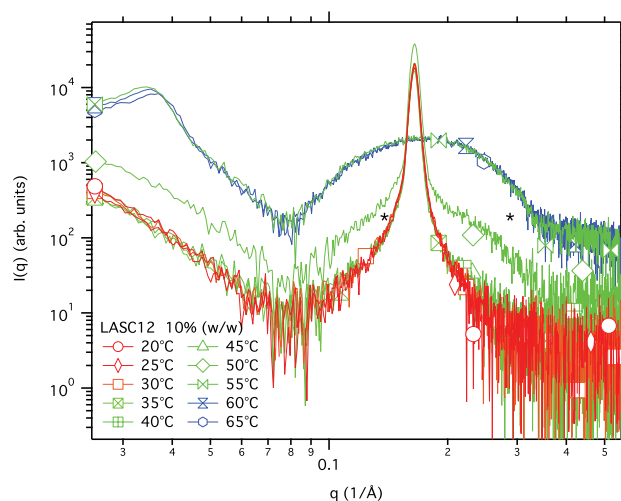

Fig. S2 Log-log representation of the SAXS scattering intensity distribution for a $w_{\text{L-ASC12}} = 10\%$ L-ASC12/water sample at: $20\,°C$ (○), $25\,°C$ (◇), $30\,°C$ (□), $35\,°C$ (⊠), $40\,°C$ (⊞), $45\,°C$ (△), $50\,°C$ (◇), $55\,°C$ (⋈), $60\,°C$ (⊠), $65\,°C$ (○). Curves are arbitrarily shifted on the y-axis to gather them in two groups: one before the transition (pure coagel state) and one after the transition (pure gel state). The broadening of the peak suggests that at $50\,°C$ both the coagel and gel coexist.
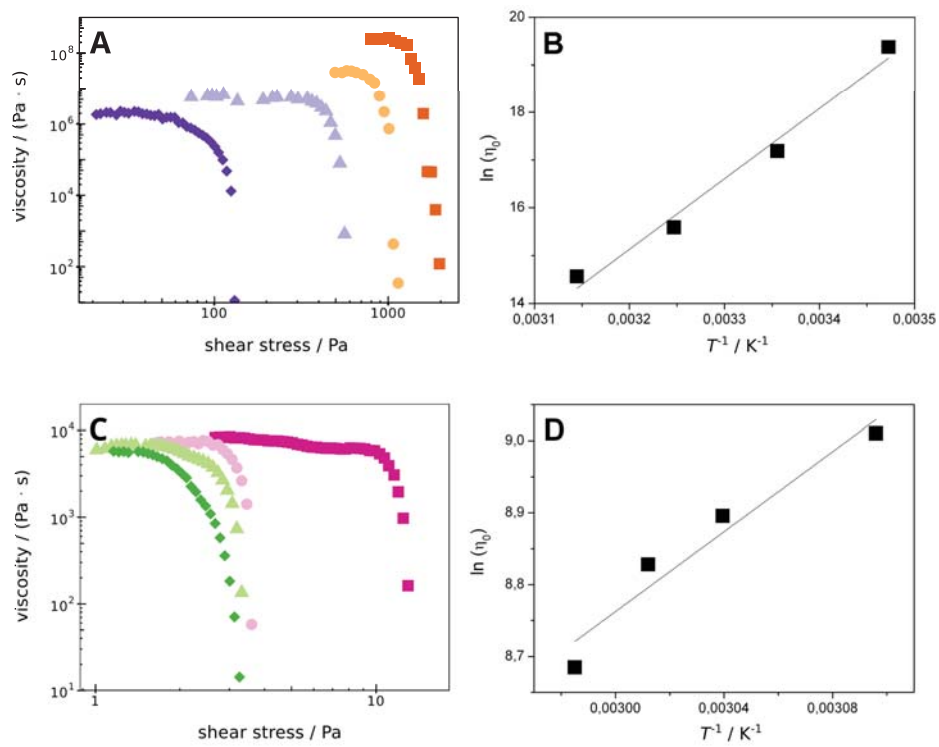
Fig. S3 A: Flow curves of a $w_{\text{L-ASC12}} = 30\%$ coagel collected at $15\,°\text{C}$ (■), $25\,°\text{C}$ (●), $35\,°\text{C}$ (▲) and $45\,°\text{C}$ (♦). B: Arrhenius plot $\ln(\eta_0)$ vs. T^{-1} obtained from the curves in A. C: Flow curves of a $w_{\text{L-ASC12}} = 30\%$ gel collected at $50\,°\text{C}$ (■), $56\,°\text{C}$ (●), $59\,°\text{C}$ (▲) and $62\,°\text{C}$ (♦). D: Arrhenius plot $\ln(\eta_0)$ vs. T^{-1} obtained from the curves in C.
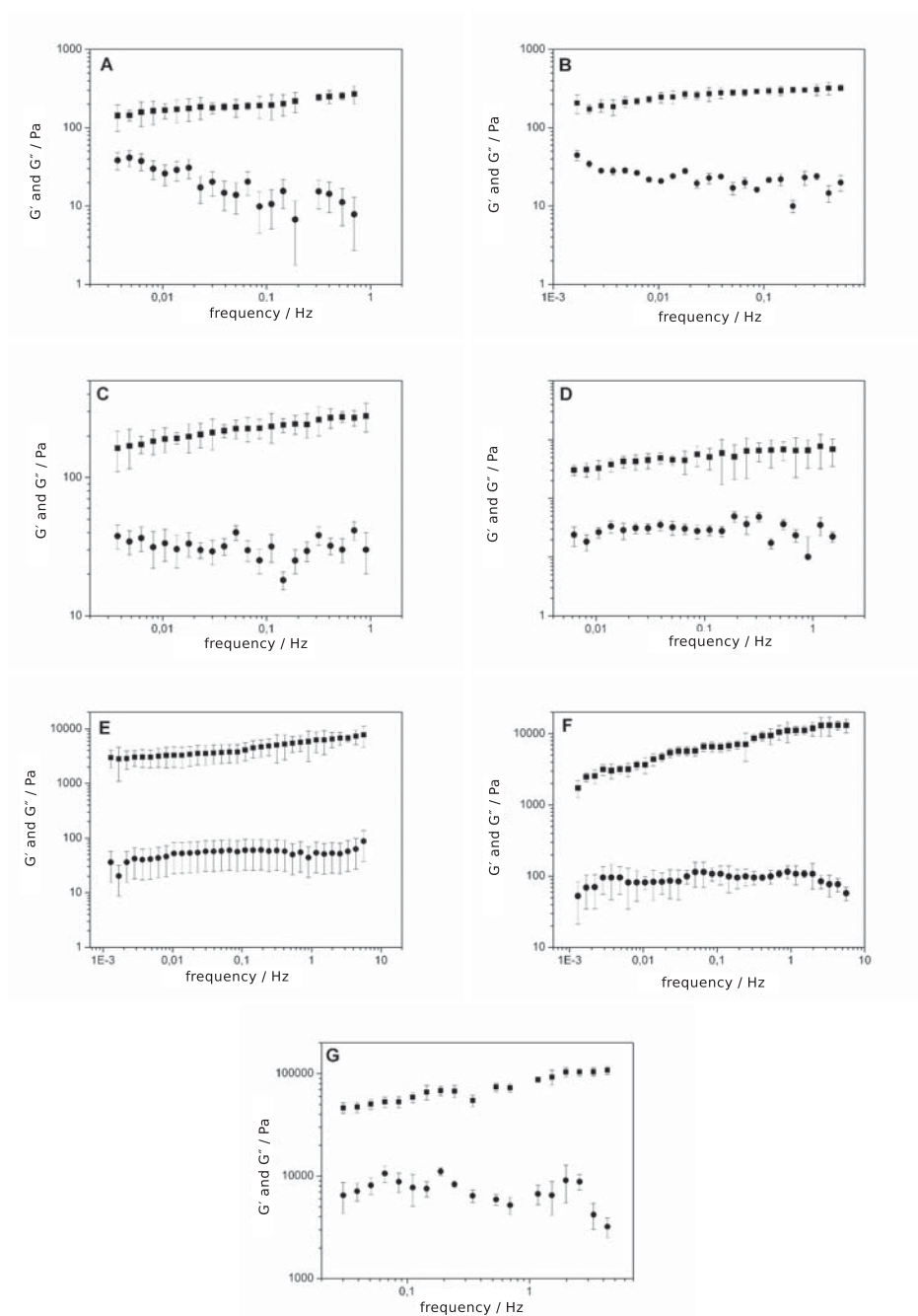
Fig. S4 Trend of the elastic modulus G' (filled squares) and of the viscous modulus G'' (filled circles) as a function of frequency for different gels at different L-ASC12 mass fractions (from A to G: 10%, 15%, 20%, 25%, 30%, 35%, 40%). The amplitude of the applied oscillating shear stress is equal to 0.1%. The error bars correspond to the standard deviation.
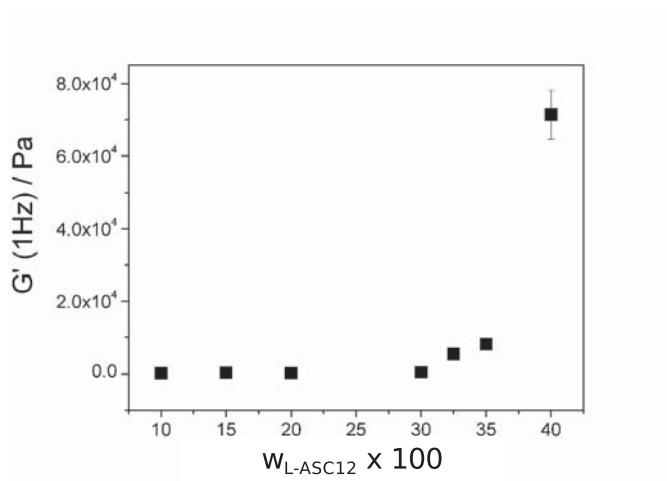
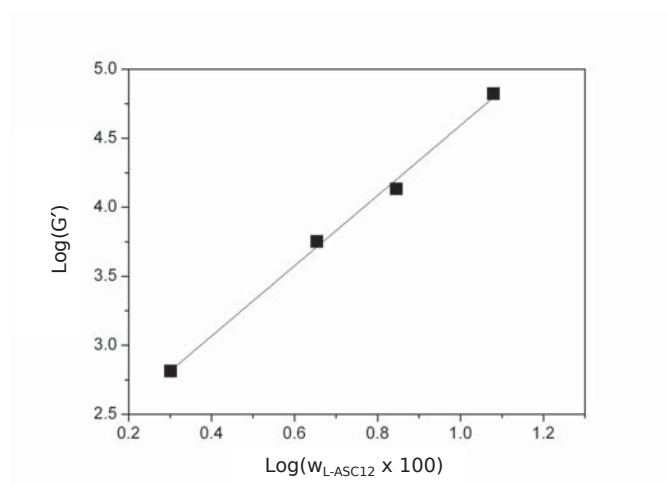**Fig. S5** Trend of the storage modulus at 1 Hz for L-ASC12 based gels at different gelator mass fractions.

Fig. S6 Value of the storage modulus G' (at the frequency of 1 Hz) as a function of L-ASC12 mass fraction.